

PHOTOEMISSION FROM Cu, Ag, AND Au IN THE 10- TO 27-eV ENERGY RANGE

D. E. Eastman and J. K. Cashion*

IBM Thomas J. Watson Research Center, Yorktown Heights, New York 10598

(Received 16 January 1970)

Measurements of high-resolution photoemission-energy distributions have been extended beyond 11.6 eV (LiF-window cutoff) for Cu, Ag, and Au. Surprisingly sharp structure ($\Delta E \sim 0.3$ eV, i.e., resonance $Q \equiv E/\Delta E \approx 50$) is resolved at these high energies. These new results show *d*-band widths of 3.0, 3.5, and 5.7 eV for Cu, Ag, and Au, respectively, and show dramatic evidence (nonstationary structure and amplitude effects) for direct transitions.

New windowless high-resolution ultraviolet-photoemission-spectroscopy (UPS) measurements at 16.8, 21.2, and 26.9 eV are reported which show much sharper structure than obtained in earlier attempts.¹⁻³ In fact, observed structure is as sharp as that observed below 11.6 eV. Increasing the range of excitation energies beyond 11.6 eV gives new information on optical selection rules and electronic structure; energy distribution curves (EDC) for Cu, Ag, and Au show much structure indicative of direct interband transitions.

These high-energy UPS measurements circumvent the usual limitation of UPS (for many materials with $h\nu < 11.6$ eV) of being able to probe the entire valence-band width. Total *d*-band widths of 3.0, 3.5, and 5.7 eV (± 0.3 eV) are observed for Cu, Ag, and Au, respectively. These widths are in good agreement with augmented plane-wave (APW) band calculations which give the observed *d*-band to Fermi-level (E_F) separations; calculated widths are 3.2 eV for Cu,⁴ 3.2 eV for Ag,⁵ and 5.8 eV for Au.⁶ Furthermore, as with x-ray photoemission spectroscopy (XPS),^{4,5} the effects of the surface-escape probability and of secondary electron emission become less important for UPS at higher photon energies (e.g., primary and secondary emission become more separated with increasing photon energy).

Photoemission measurements for Cu, Ag, and Au above 11.6 eV were made using a windowless system with a 90° cylindrical electrostatic energy analyzer having a 10-cm radius.⁷ The spectrometer resolution was determined to vary nearly linearly from 0.05 to 0.2 eV in the 0- to 20-eV kinetic-energy range. This resolution was determined by measuring the linewidth (full width at half-maximum) of the sharp $^2P_{3/2}$ line of photoionized Xe gas. Measured EDC's were corrected for the electron transmission of the spectrometer, which increases nearly linearly with increasing kinetic energy for energies > 7 eV. For energies < 7 eV, extra secondary emission due to

the spectrometer is observed.⁸

Current measurements were made using conventional counting techniques with a Bendix Channeltron electron multiplier and Hamner single-channel analyzer. The resulting spectrometer dark current was $\sim 5 \times 10^{-19}$ A (~ 3 electrons/sec). Signal currents were typically $\sim 10^{-15}$ A and complete EDC's were swept in ≤ 5 min with signal-to-noise ratios $> 50:1$.

Radiation at 21.2 eV and at 16.8 and 26.9 eV, respectively, was provided by the line spectra of cold-cathode He and Ne resonance lamps which were operated at low pressure (5 to 30 mTorr).⁹ The discharge (~ 40 mA at 1500 V) occurs in a 1-mm-diam capillary ~ 12 cm long which is optically open to the sample chamber via a 0.5-mm-diam capillary ~ 20 cm long. Two stages of differential pumping (with 4-in. glass Hg diffusion pumps) between the lamp discharge and the sample chamber are used to minimize gas throughput from the lamp. The sample chamber and electron spectrometer are pumped with an Edwards 9-in.-diam Hg diffusion pump with two chevron baffles between the pump and the sample chamber (effective speed ~ 800 liters/sec). Pressures of $\sim 3 \times 10^{-8}$ to 1×10^{-7} Torr were maintained in the sample chamber with the lamp on during all phases of the measurements; these vacuum conditions were found to yield reproducible results for Cu, Ag, and Au. Films of Cu, Ag, and Au were prepared by evaporation onto smooth Mo substrates using Mo filament evaporators.

Several EDC's for Au are shown in Fig. 1. The two EDC's for $h\nu < 11.6$ eV do not probe the full range of the *d* bands, a common limitation of UPS with LiF windows. Much observed structure is suggestive of direct transitions. The two highest energy *d*-band peaks (at ~ -2.5 eV) are seen as a 0.3-eV doublet at $h\nu = 10.2$ eV, which are split by ~ 0.6 eV at 11.6 eV.¹⁰ More dramatic shifts are seen at higher energies; e.g., the two highest-energy *d*-band peaks (at -2.6 and -3.7 eV) are split by ~ 1.1 eV at $h\nu = 16.8$ eV, by ~ 1.8 eV at $h\nu$

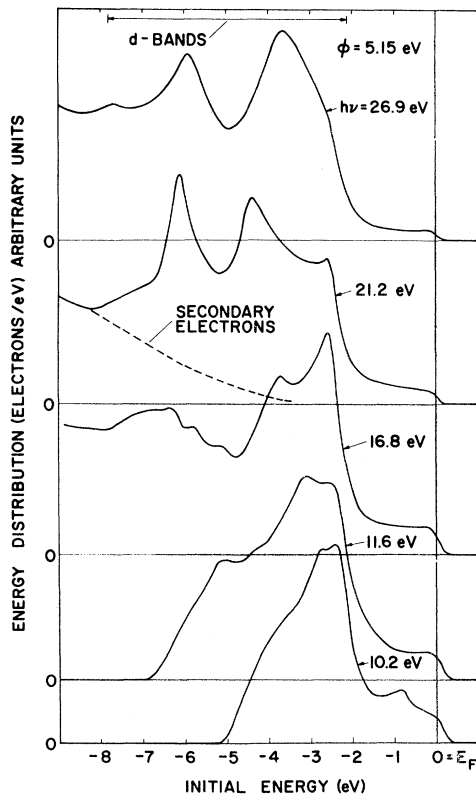


FIG. 1. Photoemission energy distributions (EDC's) for Au. All curves are plotted versus the initial-state energy, with E_F set equal to zero.

= 21.2 eV, and then move together (~ 1.1 eV separation) at $h\nu = 26.9$ eV. Three weak peaks (at -5.1 , -5.8 , and -6.3 eV) are observed in the lower half of the d -band energy region for $h\nu = 16.8$ eV, and the bottom of the bands at -7.8 eV is observed. At $h\nu = 21.2$ and 26.9 eV a sharp intense peak at ~ -6 eV dominates the emission from the lower half of the d bands. Interestingly, the over-all shape of the EDC for $h\nu = 26.9$ eV shows a similarity to XPS measurements by Siegbahn *et al.*¹¹ (two broad peaks at ~ -3.5 and -6.0 eV).

The estimated contribution of secondary emission to the measured EDC for $h\nu = 21.2$ eV is shown by the dashed line. This curve was determined by a computer analysis using the secondary-emission model of Berglund and Spicer,¹² an assumed free-electron conduction band, and an extrapolation of the scattering length $l(E)$ determined for $E < 11.6$ eV by Krolikowski and Spicer,³ who fitted the quantum yield.¹³

Sum rule calculations¹⁴ have shown that strong interband transitions from d bands persist to much higher energies than do transitions from s - p -derived bands. This behavior is shown for

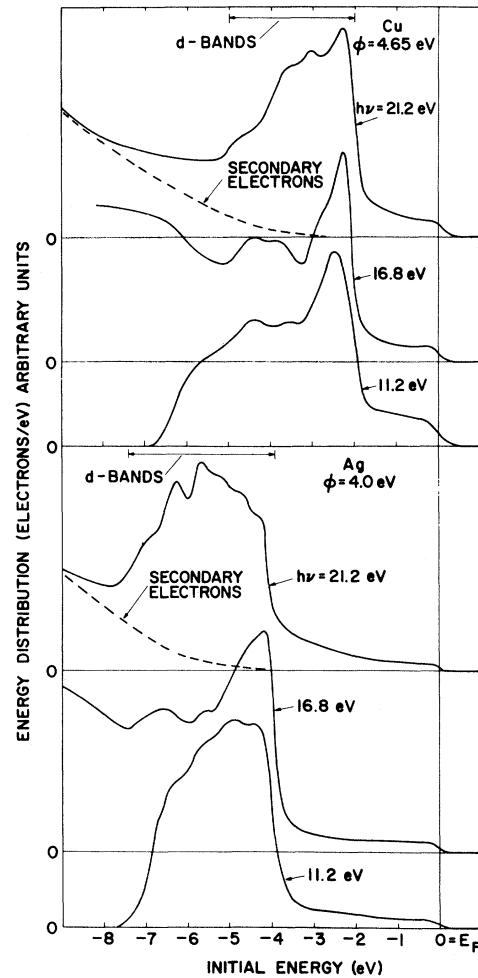


FIG. 2. Photoemission energy distributions for Cu and Ag.

Au in Fig. 1. Transitions from s - p bands within 2 eV of E_F become progressively weaker relative to d -band transitions as $h\nu$ increases from 10 to 27 eV.

EDC's for Cu are shown in Fig. 2. The d bands are observed to extend from -2.0 to -5.0 eV. Three d -band peaks (at -2.5 , -3.6 , and -4.4 eV) are resolved for $h\nu = 11.2$ eV, and the bottom of the d bands is uncertain due to scattering effects. The d -band structure becomes more resolved for $h\nu = 16.8$ eV (a sharp peak at -2.3 eV, shoulder at -2.8 eV, and two weaker peaks at -3.8 and -4.4 eV). The EDC for $h\nu = 21.2$ eV shows a different shape, with peaks at -2.3 and -3.0 eV and shoulders at -3.6 and -4.8 eV. For $h\nu = 21.2$ eV, the estimated contribution of secondary emission to the measured EDC is shown by the dashed line. This curve was determined using the above-mentioned secondary-emission model and the energy-dependent scattering length $l(E)$ determined by

Krolikowski and Spicer¹⁵ ($l \sim 22 \text{ \AA}$ at $E = 8.6 \text{ eV}$). The net primary emission from Cu (after subtraction of the calculated secondary emission) is shown in Fig. 3, where it is compared with the band density of states calculated by Mueller¹⁶ (who fit Burdick's APW band calculation⁴). In addition to strong emission from d bands between -2 and -5 eV , the data show emission from energy states between -5 and -8 eV which is consistent (both in energy and intensity) with emission from the s - p band below the bottom of the d bands. The overall shape of the d -band emission in Fig. 3 agrees surprisingly well with the density-of-states curve, and peaks at ~ -2 and -3.5 eV correlate very well. However, the observed peak at -3.0 eV occurs at a minimum in the density-of-states curve.^{17,18}

Cu was found to be more sensitive to vacuum conditions than Ag or Au. It was possible to continuously evaporate Cu during measurement of the EDC's; these results were essentially identical to those obtained within a few minutes after completion of the evaporation. Subsequent exposure to $\sim 10^{-7}$ Torr resulted in the growth of a broad emission peak due to contamination (~ 2 - 3 eV wide at $\sim -6 \text{ eV}$ below E_F) which has been previously observed¹² and was thought to be intrinsic to Cu.¹⁵

EDC's for Ag are shown in Fig. 2. The 3.5-eV -wide d bands are observed to extend from -3.9 to -7.4 eV .¹⁹ The EDC for $h\nu = 11.2 \text{ eV}$ shows structure at -4.3 , -4.9 , -5.7 and -6.3 eV . The EDC for $h\nu = 16.8 \text{ eV}$ exhibits a different shape, with a dominant peak at -4.2 eV and shoulder at -4.6 eV , and weaker structure at -5.6 and -6.6 eV . For $h\nu = 21.2 \text{ eV}$, the shape of the EDC is again different, with structure in the lower half of the d -band region (at -5.6 and -6.3 eV) being more resolved than the weak structure at -4.3 , -4.7 , and -5.2 eV .

In summary, UPS studies of Cu, Ag, and Au from 10 to 27 eV show structure as sharp as that observed below 11.6 eV , and measured d -band widths of 3.0 , 3.5 , and 5.7 eV , respectively. We observe much variation in peak locations, shapes, and amplitudes in the EDC's; such variation is inconsistent with the nondirect-transition model and a single optical density of states,¹⁵ let alone any unambiguous relation of the latter to the band density of states. If these data can be described by the direct-transition model (as suggested by recent developments^{17,20}), they contain a wealth of information concerning the one-electron model, e.g., one-electron energies $E_n(\vec{k})$, matrix

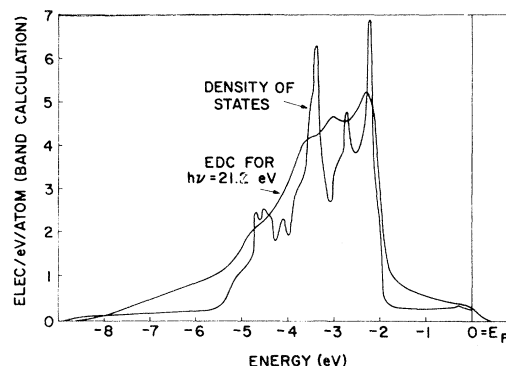


FIG. 3. The EDC for Cu at $h\nu = 21.2 \text{ eV}$ (with secondary emission subtracted) and the density of states calculated by Mueller (Ref. 16) who fit to Burdick's (Ref. 4) bands.

elements, and many-electron effects.

The technical assistance of L. W. Welsh and J. J. Donelon, and useful conversations with A. R. Williams are gratefully acknowledged.

*Present address: University of Wisconsin-Parkside, Kenosha, Wis. 53140.

¹R. C. Vehse, J. L. Stanford, and E. T. Arakawa, Phys. Rev. Letters **19**, 1041 (1967).

²R. C. Vehse and E. T. Arakawa, Oak Ridge National Laboratory Report No. ORNL-TM-2240, 1968 (unpublished).

³W. F. Krolikowski and W. E. Spicer, Phys. Rev. (to be published).

⁴G. A. Burdick, Phys. Rev. **129**, 168 (1963).

⁵E. C. Snow, Phys. Rev. **172**, 708 (1968).

⁶J. W. D. Connolly, private communication.

⁷EDC's for $h\nu \leq 11.6 \text{ eV}$ were measured using the usual arrangement, i.e., a vacuum monochromator, H_2 gas-discharge lamp, and ultrahigh-vacuum system with a LiF window for *in situ* sample preparation.

⁸This extra emission dominates the observed spectra for energies less than ~ 3 to 4 eV and prevents meaningful measurements at these low energies.

⁹The 26.9-eV line of Ne is accompanied by two satellite lines at 27.8 and 30.5 eV which have relative intensities of 20 and 5% , respectively. The effects of these satellite lines were subtracted from the EDC for 26.9 eV (assuming no change in line shape).

¹⁰This splitting has also been observed in UPS measurements on cesiated Au by P. O. Nilsson *et al.*, to be published.

¹¹K. Siegbahn *et al.*, Electron Spectroscopy for Chemical Analysis, Atomic, Molecular, and Solid State Structure Studied by Means of Electron Spectroscopy (Almqvist and Wiksells Boktryckeri AB, Uppsala, Sweden, 1967), Ser. IV, Vol. 20.

¹²C. N. Berglund and W. E. Spicer, Phys. Rev. **136**, A1030, A1044 (1964).

¹³The magnitude of the scattering shown in Fig. 1 was

increased by $\sim 15\%$ from the calculated value in order to delineate more clearly the bottom of the d band at ~ -7.8 eV.

¹⁴H. Ehrenreich, H. R. Philipp, and B. Segall, *Phys. Rev.* **132**, 1918 (1963).

¹⁵W. F. Krolkowski and W. E. Spicer, *Phys. Rev.* **185**, 882 (1969).

¹⁶F. M. Mueller, *Phys. Rev.* **153**, 659 (1967).

¹⁷N. V. Smith and W. E. Spicer, *Opt. Commun.* **1**, 157 (1969), have recently shown that UPS data for Cu for $h\nu < 11.6$ eV can be described by direct transitions.

¹⁸N. V. Smith, in *Proceedings of the Symposium on the Electronic Density of States*, Washington, D. C., 3-6 November 1969 (to be published), has observed direct transitions in cesiated Cu for $6 \lesssim h\nu \lesssim 8$ eV.

¹⁹The EDC's previously reported for Ag (Ref. 1) are consistent in overall shape with those shown in Fig. 2, but did not resolve d -band structure.

²⁰J. Janak, D. E. Eastman, and A. R. Williams, in *Proceedings of the Symposium on the Electronic Density of States*, Washington, D. C., 3-6 November 1969 (to be published).

NEAREST-NEIGHBOR MODEL OF MAGNETISM FOR COPPER-NICKEL ALLOYS AND CLUSTERING OF MAGNETIC MOMENTS

J. P. Perrier, B. Tissier, and R. Tournier

Centre de Recherches sur les Très Basses Températures, Centre National de la Recherche Nucleaire,
Cedex 166, 38 Grenoble, France
(Received 24 November 1969)

We show that the appearance of a localized moment on Ni atoms in the critical range of concentration is accurately described by a simple environment-dependent model of the Jaccarino-Walker type, and that this model implies a "clustering" of magnetic moments, even on the basis of a random distribution of atoms. The fit with experimental data is promising in view of the approximations made.

Copper-nickel alloys have been extensively studied, particularly in the "critical range" of concentrations between 30 and 60 at.% Ni. High-temperature susceptibility measurements¹ show a strong increase of the susceptibility with concentration, which leads to the supposition of the existence of superparamagnetism. In saturation-moment measurements,^{2,3} the plot of the magnetization versus the concentration x of the Ni atoms, linear for $x > 0.6$, exhibits a curvature for $x < 0.6$. This peculiarity has not yet been explained in a satisfactory manner, in spite of several attempts.^{4,5} Moreover, the experimental values of σ_s deduced in different ways for the same sample do not agree with one another.³ Low-temperature specific-heat measurements^{3,6} show two anomalies from the usual $c = \gamma T + \beta T^3$ law. The behavior of the specific heat versus temperature is well fitted by the law $c = A + \gamma T + \beta T^3$, A and γ being concentration dependent. Moreover, neutron diffraction patterns have shown the existence of giant moments in Ni-Cu alloys, even in the ferromagnetic range.⁷

All these results have been qualitatively explained by the cluster hypothesis: The nickel atoms tend to cluster into Ni-rich regions in which they can be magnetically coupled; these regions behave like giant moments and give rise to superparamagnetism and anomalies in the specific

heat.⁸ Although this interpretation has recently been contested, it can be said that no available facts invalidate the model.⁸

Consistent with the cluster hypothesis are the measurements of the effects of heat treatment, plastic deformation, and neutron irradiation on Cu-Ni alloys.^{1,3,9}

The short-range order parameters defining the rate of clustering have been correlated with the values of the susceptibilities.¹⁰ There is no doubt now that an alloy slowly cooled from high annealing temperature is not randomly distributed, as shown recently.¹¹ It could be expected that a perfectly random state never occurred, and that short-range order parameters¹² were necessary to describe the statistical properties of the alloy.⁵ However, experiments by one of us⁹ tend to show that no short-range order exists at room temperature if the samples are annealed long enough at a temperature higher than 400°C and are very rapidly quenched. It was shown with magnetic measurements that the metastable state obtained from annealing temperatures between 400 and 1000°C seemed to be the same. If there were any short-range order, such a thing could not occur since this phenomenon depends on temperature. Our purpose is, then, to explain the main physical properties of Cu-Ni alloys in the critical range on the basis of a pure-